

May 2004

Effects of Fermion Masses and Twisting on Non-Integrable Phases on Compact Extra Dimensions

Müge Boz^a and Namık K. Pak^b

^a *Department of Physics, Hacettepe University, Turkey, TR06800*

^b *Department of Physics, Middle East Technical University, Turkey, TR06531*

Abstract

The effective potential for the Wilson loop in the SU(2) gauge theory with N_f massive fundamental and N_a massive adjoint fermions on $S^1 \times M^4$ is computed at the one-loop level, assuming periodic boundary conditions for the gauge field and general boundary conditions for fermions. It is shown that there are critical values for the bare mass, and the boundary condition parameter for the adjoint fermions, beyond which the symmetry pattern changes. However, neither bare mass, nor the boundary condition parameter for the fundamental fermion play any role on the vacuum structure, thus the symmetry breaking pattern. When the two different types of fermions with equal masses exist together the pattern of the fundamental fermion dominate, and SU(2) gauge symmetry remains intact independent of the fermion masses.

arXiv:hep-ph/0402238v2 17 Aug 2004

1 Introduction

It has long been known that gauge theories on multiply-connected spaces exhibit anomalous behavior in that the gauge connection is promoted to a physical observable. The simplest example is provided by Aharonov-Bohm effect [1] according to which the interference of matter waves in the presence of an impenetrable domain of magnetic field is modulated by the magnetic flux. This observation has later been furthered [2] to prove the dynamical nature of the connection and the irrelevance of single-valuedness of the matter and gauge fields. The analysis of [2], which was focused on massless fermions in the fundamental representation of the gauge group, has subsequently been generalized to adjoint fermions [3, 4, 5]. Recently, effects of adjoint fermion masses have been incorporated into the previous works [6], and it was pointed out that there exist certain critical values of the fermion masses across which the symmetries of the system change.

For appreciating the importance of the Wilson loop dynamics, consider for definiteness a gauge theory in a 5-dimensional factorizable geometry $M^4 \times S^1$ where S^1 is a circle with radius R . The gauge field A_B ($B = (\mu, y), \mu = 0, 1, 2, 3$) has five independent components, and it is forbidden to have any local potential due to higher dimensional gauge invariance. However, the non-integrable phase factor

$$\theta(x) = -i \ln \left[P e^{i \int_{y=0}^{y=2\pi R} dy A_y(x_\mu, y)} \right], \quad (1)$$

being inherently non-local in the direction of extra dimension, develops a non-local potential in the presence of charged bulk fields. In case $\theta(x)$ develops a nonvanishing vacuum expectation value (VEV) the gauge symmetry can be broken dynamically depending on the model parameters [5]. This has been particularly useful in string compactifications [7]. Furthermore, recently it has been pointed out that radiatively-lifted vanishing potential for the non-integrable phase factor $\theta(x)$ makes it a perfect candidate for inflaton [8, 9, 10] which has to acquire an extremely flat potential to comply with the requirements of successful inflation.

In this work, we consider a non-supersymmetric SU(2) gauge model with N_f massive adjoint fermions, and N_a massive fundamental fermions, with the most general boundary condition parameters for the fermions and the gauge fields on $S^1 \times M^4$. Here is a brief summary of the present work in relation with the previous works:

Hosotani has previously considered a SU(2) gauge theory defined both on $S^1 \times R^1$ and $S^1 \times M^3$ with massless fermions, but with arbitrary boundary condition (bc) parameters for the gauge fields, and fermions [5]. He has shown that the SU(2) gauge symmetry is not broken, when the fermions are in the fundamental representation (FR), irrespective of the values of the bc parameters¹. But the SU(2) symmetry breaks down to U(1) for certain values of the bc parameter below a certain critical value, for the adjoint representation (AR). Takenaga more recently considered an SU(2) gauge theory $S^1 \times M^4$ with massive adjoint fermions, with periodic boundary conditions for fermions [6]. He has shown that below a certain critical value of the bare mass the symmetry again breaks down to U(1).

In Section 3, we considered a SU(2) gauge theory with massive adjoint fermions and with arbitrary bc parameters. We have shown that below certain critical values of the bare mass and bc parameter the symmetry breaks down to U(1), and agrees with the results of Hosotani and Takenaga, respectively, in the corresponding limits.

¹In more detail, for $\delta_f < \pi/2$, absolute minimum is located at $\theta_m = \pi$, corresponding to $U^{sym} = -I$, and for $\pi/2 < \delta_f < \pi$, the absolute minimum is located at $\theta_m = 0$, corresponding to $U^{sym} = I$. Both of these U^{sym} are elements of the center of SU(2), thus the SU(2) symmetry is unbroken.

In Section 4, we extended this discussion in [5] for massless fundamental fermions, by including bare masses for fermions. We have shown that neither bc parameter δ_f , nor the bare mass for the fundamental fermion play any role on the vacuum structure/symmetry breaking pattern.

Finally, in Section 5, we considered the general case with N_f fundamental and N_a adjoint fermions with equal masses. We have observed that the fundamental fermions play a more dominant role than the adjoint ones, on the gauge symmetry pattern, as the result turns out to be very similar to the pure fundamental fermions case.

2 The Effective Potential

Consider an SU(2) gauge theory on $M^4 \times S^1$ with N_a adjoint and N_f fundamental fermions. The action is completely fixed by gauge invariance

$$S = \int d^4x dy \left[-\frac{1}{2g_5^2} \text{tr} \{F_{AB}F^{AB}\} + \bar{\psi} (\gamma^A D_A - m_f) \psi + \bar{\lambda} (\gamma^A D_A - m_a) \lambda \right], \quad (2)$$

where ψ and λ stand, respectively, for fundamental and adjoint fermion fields with masses m_f and m_a , and g_5 , with dimension of $(\text{mass})^{-1/2}$, is the higher dimensional gauge coupling. The potential for A_5 is perfectly flat since gauge invariance forbids the induction of any local operator which can lift the flatness. However, the phase of the Wilson loop $\theta(x)$ is inherently non-local in the extra dimension and thus it can acquire a non-trivial non-local potential. Indeed, the gauge field kinetic term in (2), after dimensional reduction, generates the kinetic term

$$\mathcal{L}_{KK}^{(4)} = \frac{1}{2L^2 g_4^2} \sum_a (\partial_\mu \theta^a)^2, \quad (3)$$

where $g_4 = \frac{g_5}{\sqrt{2\pi R}}$ is the four dimensional gauge coupling constant, and we defined a new field such that

$$\theta^a(x) = g_5 \int_0^{2\pi R} dy A^{5,a}(x, y) = 2\pi R g_5 A^{5,a}(x) = L g_5 A^{5,a}(x), \quad (4)$$

using the compactness of S^1 which guarantees the y -independence of the zero mode $A^{5,a}(x, y)$. However, the exactly flat potential of (3) is lifted by the gauge boson and fermion loops. This radiative contribution, denoted by V_{af} , is given by

$$\begin{aligned} V_{af}(\theta, N_a, N_f, z_a, z_f, \delta_a, \delta_f) &= \frac{1}{c_1} \left\{ -3 \sum_{n=1} \frac{1}{n^5} \left[1 + \cos 2n\theta \right] \right. \\ &+ 2 N_a \sum_{n=1} \frac{F(z_a n)}{n^5} \left[2 \cos n\delta_a + \cos n(2\theta + \delta_a) + \cos n(2\theta - \delta_a) \right] \\ &\left. + 2 N_f \sum_{n=1} \frac{F(z_f n)}{n^5} \left[\cos n(\theta + \delta_f) + \cos n(\theta - \delta_f) \right] \right\}, \quad (5) \end{aligned}$$

where

$$F(zn) = e^{-zn} \left[1 + zn + \frac{1}{3} z^2 n^2 \right] \quad \text{with} \quad z = mL, \quad (6)$$

and

$$\frac{1}{c_1} = \frac{3}{2\pi^2 L^5}. \quad (7)$$

Here, the θ is related to θ^a in Eq. (4), through the relationship:

$$Lg_5 A_5^a \tau^a = \theta^a \tau^a = C \begin{pmatrix} \theta & 0 \\ 0 & -\theta \end{pmatrix} C^+, \quad (8)$$

with the constant 2×2 matrix satisfying $C^+ C = I$, and $\theta = \sqrt{\theta_1^2 + \theta_2^2 + \theta_3^2}$. We would like to point out, following Hosotani [5], that because of the invariance of the boundary conditions under global gauge transformations the effective potential does not depend on C , and for the $SU(2)$ case depends only on the single θ and the phases of the fermions.

In (5), the first line follows from the gauge and the ghost fields, and the second and the third lines are the contributions of N_a massive adjoint and N_f massive fundamental fermions, respectively. The expression (5) reduces correctly to various special cases already discussed in the literature [2, 3, 4, 5, 6]. One notes that the phases δ_a , and δ_f are defined through the boundary conditions. As S^1 is not simply connected, boundary conditions must be specified for the single valuedness of the observables. For the gauge field we adopt periodic boundary conditions; for the fermion fields we impose the following general boundary conditions:

$$\begin{aligned} \psi_f(x, y + L) &= e^{i\delta_f} \psi_f(x, y) , \\ \psi_a(x, y + L) &= e^{i\delta_a} \psi_a(x, y) . \end{aligned} \quad (9)$$

In what follows we discuss the three specific cases of adjoint, fundamental and adjoint plus fundamental fermions separately. In each case we analyze the potential landscape both analytically and numerically with the aim of determining if the original gauge symmetry is respected by the effective potential (5).

3 The case with Adjoint Fermions only

We first consider the case which there are N_a massive adjoint fermions with the phases δ_a . The effective potential takes the form

$$V_a(\theta, N_a, z_a, \delta_a) = \frac{1}{c_1} \sum_{n=1} \frac{1}{n^5} \left[-3 + 4 N_a F(z_a n) \cos n\delta_a \right] \left[1 + \cos 2n\theta \right], \quad (10)$$

Note that the effective potential reduces to that of N_a massless adjoint fermions with phases δ_a when $z \rightarrow 0$ [5], and differs from the model considered by Takenaga [6] by the $\cos n\delta_a$ term multiplying F_a .

To identify the role played by the massive fermions with phase δ_a on the vacuum structure, we have to look at the two special limits, namely $z_a \rightarrow \infty$, and $z_a \rightarrow 0$. The behaviour in the first case is identical to that of Takenaga [6], as the fermion is decoupled in this case. The dominant contribution comes from the gauge sector, and the vacuum configuration is given by $\theta = 0 \pmod{\pi}$ independent of δ_a . Clearly, the $SU(2)$ gauge symmetry is not broken in this case. In the massless limit, $z_a \rightarrow 0$, let us note that when $\delta_a = 0$, the vacuum configuration is given by $\theta = \pi/2 \pmod{\pi}$ [4]. However when $\delta_a \neq 0$, we will see that there exists a critical value δ_a^c , above which $\theta = 0 \pmod{\pi}$ is an absolute minimum. To find the critical value $\delta_c^{(a)}$, we define:

$$c_2 V_a''(\theta = 0 \pmod{\pi}, N_a, z_a = 0, \delta_a) = \sum_{n=1} \frac{1}{n^3} \left[3 - 4 N_a \cos n \delta_a \right], \quad (11)$$

where

$$c_2 = \frac{c_1}{4}, \quad (12)$$

and we have used the standard definitions:

$$\begin{aligned} \sum \frac{\cos n\pi}{n^D} &= -\left[1 - 2^{(-D)}\right] \xi_D, \text{ and} \\ \xi_D &= \sum \frac{1}{n^D}, \end{aligned} \quad (13)$$

We plot $c_2 V_a''(\theta = 0 [\text{mod } \pi], N_a = 1, z_a = 0, \delta_a)$ with respect to δ_a in Figure 1. As can be seen from Figure 1 that there is a critical value at $\delta_a^{c1} = 0.53$.

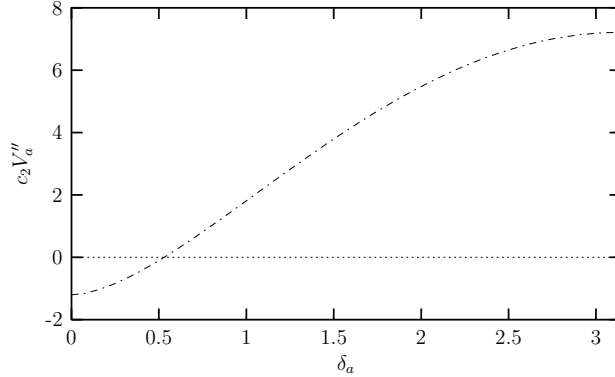


Figure 1: The δ_a dependence of $c_2 V_a''(\theta = 0 [\text{mod } \pi], N_a = 1, z_a = 0, \delta_a)$.

Consistency with the results of Davies and McLachan [4] requires that there must be a critical value (same or different than δ_a^{c1}) below which $\theta = \pi/2 [\text{mod } \pi]$ is an absolute minimum. To find this critical value, we again define

$$c_2 V_a''(\theta = \pi/2 [\text{mod } \pi], N_a, z_a = 0, \delta_a) = \sum_{n=1} \frac{(-1)^n}{n^3} \left[3 - 4 N_a \cos n\delta_a \right], \quad (14)$$

and in Figure 2, we investigate the dependence of $c_2 V_a''(\theta = \pi/2 [\text{mod } \pi], N_a = 1, z_a = 0, \delta_a)$ on δ_a .

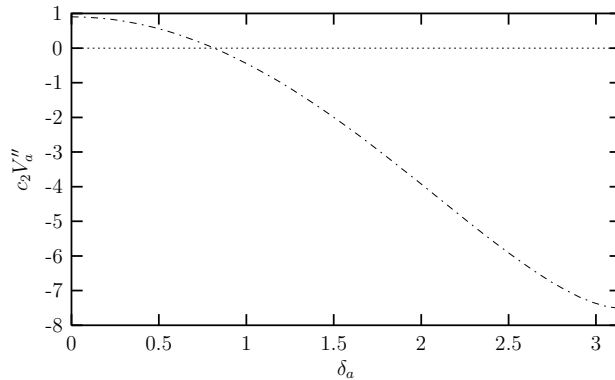


Figure 2: The δ_a dependence of $c_2 V_a''(\theta = \pi/2 [\text{mod } \pi], N_a = 1, z_a = 0, \delta_a)$.

As can be seen from Figure 2 that there is a critical point at $\delta_a^{c2} = 0.81$, which is different from the previous case.

If we summarize,

(i) For $\delta_a^{c2} < \delta_a < \pi$, $\theta = 0 \pmod{\pi}$ is an absolute minimum, and the SU(2) gauge symmetry is not broken.

(ii) For $0 < \delta_a < \delta_a^{c1}$, $\theta = \pi/2 \pmod{\pi}$ is an absolute minimum, and the gauge symmetry is dynamically broken down to U(1).

This observation suggests that there must exist certain critical values of z_a at which gauge symmetry breaking patterns change when $0 < \delta_a < \delta_a^{c1}$ (note that this does not happen when $\delta_a^{c2} < \delta_a < \pi$, as there is no difference in the symmetry breaking structure from $z_a \rightarrow \infty$ to $z_a \rightarrow 0$).

Before addressing the stability question of the vacuum configurations identified above, we would like to study the interval $\delta_a^{c1} < \delta_a < \delta_a^{c2}$ in detail. Figure 1 and Figure 2 suggest that in this interval of δ_a all the three vacuum configurations, namely $\theta = 0, \pi/2$ exist simultaneously. The behaviour of $c_1 V_a(\theta, N_a = 1, z_a = 0, \delta_a)$ for different values of δ_a in this interval is plotted in Figure 3.

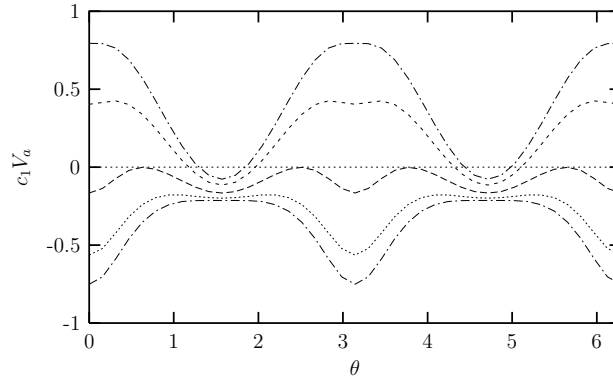


Figure 3: The dependence on θ of $c_1 V_a(\theta, N_a = 1, z_a = 0, \delta_a)$. Here, the top and bottom dot-dashed curves represent $\delta_a^{c1} = 0.53$, and $\delta_a^{c2} = 0.81$ values of δ_a respectively, whereas the three different curves in the $\delta_a^{c1} < \delta_a < \delta_a^{c2}$ interval correspond to $\delta_a = 0.61, 0.71, 0.78$, from top to bottom, respectively.

We see from Figure 3 that for δ_a close to δ_a^{c2} , $\theta = 0 \pmod{\pi}$ and δ_a close to δ_a^{c1} , $\theta = \pi/2 \pmod{\pi}$ are the absolute minima, respectively. Somewhere in between, namely at $\delta_a = 0.71$, the two are degenerate. That is in the massless case, for the values of δ_a within the interval $(\delta_a^{c1}, \delta_a^{c2})$, there exists a mixed phase, namely unbroken SU(2) phase together with the broken phase U(1). This interesting phenomena clearly deserves further study, which we postpone to a future work.

To confirm the existence of the critical values of z_a we have to study the stability of the configurations $\theta = 0 \pmod{\pi}$, and $\theta = \pi/2 \pmod{\pi}$ with respect to z_a , corresponding to vacuum configurations, in the limits $z_a \rightarrow \infty$ as well as $z_a \rightarrow 0$ (when $\delta_a^{c2} < \delta_a < \pi$), and $z_a \rightarrow 0$ (when $0 < \delta_a < \delta_a^{c1}$), respectively.

The second derivative of the effective potential is plotted with respect to z_a for $\theta = 0 \pmod{\pi}$ in Figure 4, and for $\theta = \pi/2 \pmod{\pi}$ in Figure 5, for $N_a = 1$, with their explicit expressions given as :

$$\begin{aligned}
 c_2 V_a''(\theta = 0 \pmod{\pi}, N_a, z_a, \delta_a^{c2} < \delta_a < \pi) &= 3\xi_3 - 4 N_a \sum_{n=1} \frac{F(z_a n) \cos n\delta_a}{n^3}, \\
 c_2 V_a''(\theta = \pi/2 \pmod{\pi}, N_a, z_a, 0 < \delta_a < \delta_a^{c1}) &= -\frac{9}{4}\xi_3 - 4 N_a \sum_{n=1} \frac{(-1)^n F(z_a n) \cos n\delta_a}{n^3}, \quad (15)
 \end{aligned}$$

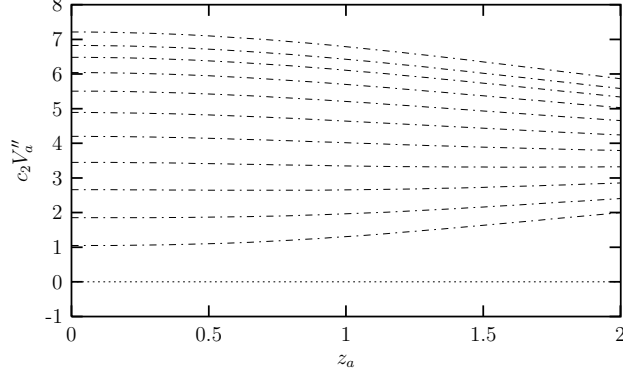


Figure 4: The z_a dependence of $c_2 V_a''(\theta = 0 [\text{mod } \pi], N_a = 1, z_a, \delta_a^{c1} < \delta_a < \pi)$. Here, $\delta_a^{c2} = 0.81$ for the bottom curve, whereas $\delta_a = \pi$ for the top curve.

We see from Figure 4 that $c_2 V_a''(\theta = 0, N_a = 1, z_a, \delta_a^{c2} < \delta < \pi)$ is always positive, and there is no critical value z_a^c where V_a'' changes sign, and $\theta = 0 [\text{mod } \pi]$ is stable independent of z_a . This is consistent with the previous observation that as long as $\delta_a^{c2} < \delta_a < \pi$, $\theta = 0 [\text{mod } \pi]$ is an absolute minimum both in $z_a \rightarrow \infty$ and $z_a \rightarrow 0$ limits.

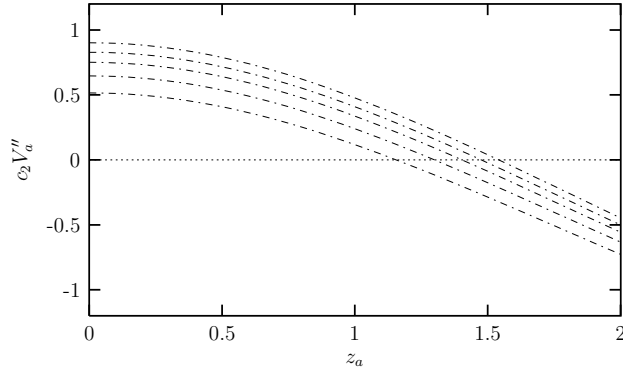


Figure 5: The z_a dependence of $c_2 V_a''(\theta = \pi/2 [\text{mod } \pi], N_a = 1, z_a, 0 < \delta < \delta_a^{c1})$. Here, $\delta_a = 0$ for the top curve, whereas $\delta_a^{c1} = 0.53$ for the bottom curve.

We see from Figure 5 that there are critical values for z_a , depending on the values of δ_a , below which $V_a''(\theta = \pi/2, N_a = 1, z_a, 0 < \delta < \delta_a^{c1})$ is positive. The largest of these z_a^c corresponding to $\delta_a = 0$ is $z_a^c = 1.5$, which is identical to the result of Takenaga [6]. The larger δ_a is, within the allowed range $(0, \delta_a^{c1})$, the smaller z_a gets. That is, the symmetry breaking pattern is more sensitive to adjoint mass for larger values of the phase δ_a , in the allowed range $(0, \delta_a^{c1})$.

If we summarize

(i) when $0 < \delta_a < \delta_a^{c1}$, $V_a''(\theta = \pi/2, N_a = 1, z_a, \delta_a) > 0$ for a set of values for $z_a < z_a^c = 1.5$, the gauge symmetry is broken to $U(1)$,

(ii) when $\delta_a^{c2} < \delta_a < \pi$, $V_a''(\theta = 0 [\text{mod } \pi], N_a = 1, z_a, \delta_a) > 0$, independent of the values of z_a , and the gauge symmetry $SU(2)$ is intact.

(iii) when $\delta_a^{c2} < \delta_a < \delta_a^{c1}$, there exists a mixed phase, namely the unbroken $SU(2)$ phase together with the broken phase $U(1)$.

For instance, in Figure 6, we show the z_a dependence of $c_2 V_a''(\theta = \pi/2 [\text{mod } \pi], N_a = 1, z_a, \delta_a)$ when $\delta_a = 0.71$, for which case the two minima are degenerate (see Figure 3), with the critical

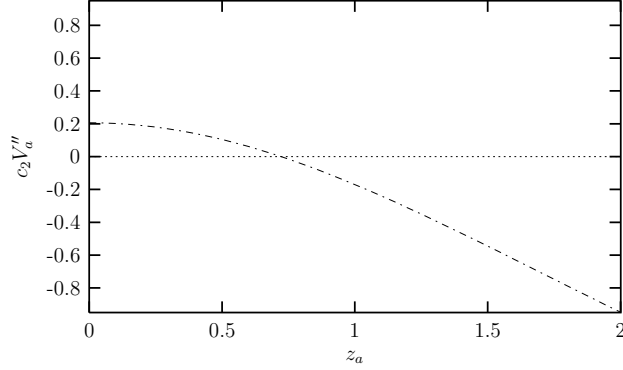


Figure 6: The z_a dependence of $c_2 V_a''(\theta = \pi/2 [\text{mod } \pi], N_a = 1, z_a, \delta_a = 0.71)$.

value $z_c = 0.72$. We would have obtained identical information if we have plotted $c_2 V_a''(\theta = 0 [\text{mod } \pi], N_a = 1, z_a, \delta_a = 0.71)$.

4 The Case with Fundamental fermions only

When there are N_f massive fundamental fermions only, with the bc phases δ_f , the potential takes the form:

$$V_f(\theta, N_f, z_f, \delta_f) = \frac{1}{c_1} \sum_{n=1} \frac{1}{n^5} \left[-3(1 + \cos 2n\theta) + 4 N_f F(z_f n) \cos n\delta_f \cos n\theta \right]. \quad (16)$$

The effective potential reduces to that of N_f massless fundamental fermions with phases δ_f [2, 5] in the $z_f \rightarrow 0$ limit. Again, to identify the role played by the masses and the δ_f -phases of the fermion on the vacuum structure, we have to look at the $z_f \rightarrow \infty$, and $z_f \rightarrow 0$ limits. As the fermions decouple in the former case, this case is identical to that of adjoint fermions, and the vacuum structure is given by $\theta = 0 [\text{mod } \pi]$ independently of δ_f . The SU(2) gauge symmetry is intact in this regime.

Next, we look at the $z_f \rightarrow 0$ limit, in detail. First recall that this limit with $\delta_f \neq 0$ was considered by Hosotani [2], for $M^3 \times S^1$. He has shown that the absolute minimum is $\theta = 0$, for $\pi/2 < \delta_f < \pi$, and $\theta = \pi$ for $0 < \delta_f < \pi/2$ independent of the number of fermions N_f ; furthermore these two absolute minima are degenerate for $\delta_f = \pi/2$. He has further shown, as mentioned before in the footnote, that in both cases the gauge symmetry is unbroken. We have $M^4 \times S^1$; therefore the critical value of δ_f (δ_f^c), if there is any, could be different than that of Hosotani [2]. We first plot the expressions for $V_f''(\theta = 0, N_f, z_f = 0, \delta_f)$, and $V_f''(\theta = \pi, N_f, z_f = 0, \delta_f)$, to identify the δ_f -regions where $\theta_m = 0, \pi$ are the minima, respectively.

Using (16), we get:

$$\begin{aligned} c_2 V_f''(\theta = 0, N_f, z_f = 0, \delta_f) &= \sum_{n=1} \frac{1}{n^3} \left[3 - N_f \cos n\delta_f \right], \\ c_2 V_f''(\theta = \pi, N_f, z_f = 0, \delta_f) &= \sum_{n=1} \frac{1}{n^3} \left[3 - N_f (-1)^n \cos n\delta_f \right], \end{aligned} \quad (17)$$

and analyze the dependence on δ_f of $c_2 V_f''(\theta = 0, N_f, z_f = 0, \delta_f)$ and $c_2 V_f''(\theta = \pi, N_f, z_f = 0, \delta_f)$ in Figure 7 and Figure 8, respectively when $N_f = 1, 2, 3, 4$.

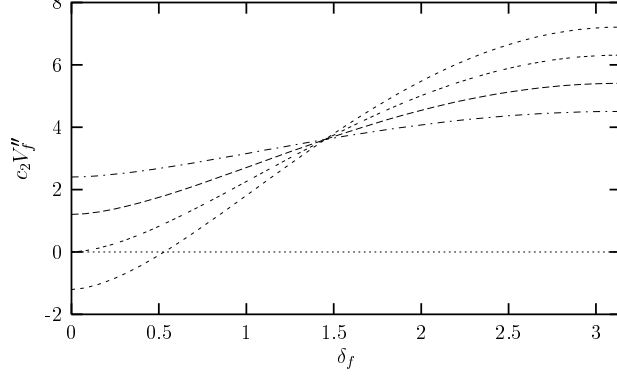


Figure 7: The δ_f dependence of $c_2 V_f''(\theta = 0, N_f, z_f = 0, \delta_f)$, when $N_f = 1$ (top curve), and $N_f = 4$ (bottom curve). The curves in between are for $N_f = 2, N_f = 3$, from top to bottom.

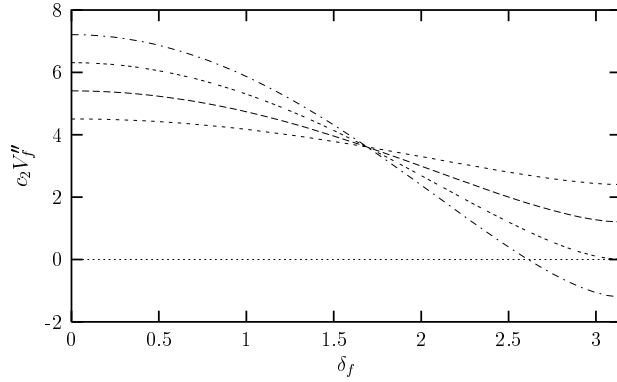


Figure 8: The δ_f dependence of $c_2 V_f''(\theta = \pi, N_f, z_f = 0, \delta_f)$, when $N_f = 1$ (bottom curve) and $N_f = 4$ (top curve). The curves in between are for $N_f = 2, N_f = 3$, from bottom to top.

A comparative look at Figure 7 and Figure 8 suggests that $c_2 V_f''(\theta = 0, N_f, z_f = 0, \delta_f)$ and $c_2 V_f''(\theta = \pi, N_f, z_f = 0, \delta_f)$ do not change sign with the variation of δ_f for $N_f = 1, 2$, whereas they change sign for $N_f = 4$ (the bottom curve in Figure 7, and the top curve in Figure 8).

To verify that N_f indeed plays a role on the structure of the minima, we study the sign of $V_f''(\theta, N_f, z_f = 0, \delta_f)$ at the limits of δ_f for each $\theta = 0$, and $\theta = \pi$ as a function of N_f ($\theta = 0, \pi$ corresponding to the limits of periodic, and antiperiodic boundary conditions):

$$\begin{aligned}
 c_2 V_f''(\theta = 0, N_f, z_f = 0, \delta_f = 0) &= \left\{ \left(3 - N_f \right) \xi_3 \right\} > 0 \text{ for } N_f = 1, 2, \\
 &< 0 \text{ for } N_f \geq 4, \\
 c_2 V_f''(\theta = \pi, N_f, z_f = 0, \delta_f = \pi) &= \left\{ \left(3 - N_f \right) \xi_3 \right\} > 0 \text{ for } N_f = 1, 2, \\
 &< 0 \text{ for } N_f \geq 4, \tag{18}
 \end{aligned}$$

and

$$\begin{aligned}
 c_2 V_f''(\theta = 0, N_f, z_f = 0, \delta_f = \pi) &= \left\{ \frac{3}{4} \xi_3 (N_f + 4) \right\} > 0 \text{ for all } N_f, \\
 c_2 V_f''(\theta = \pi, N_f, z_f = 0, \delta_f = 0) &= \left\{ \frac{3}{4} \xi_3 (N_f + 4) \right\} \gtrsim 0 \text{ for all } N_f. \tag{19}
 \end{aligned}$$

One notices that for $N_f \geq 4$ case there are some subtleties, and thus we pay special attention to $N_f = 4$:

We see from Figure 7 that there is a critical value $\delta_a^{c1} = 0.53$, above which $c_2 V''(\theta = 0, N_f, z_f = 0, \delta_f = 0) > 0$. Moreover as Figure 8 suggests there is another critical value $\delta_a^{c2} = 2.61$ which is different from the former case, below which $c_2 V_f''(\theta = \pi, N_f, z_f = 0, \delta_f = 0) > 0$. Thus, for $N_f = 4$, the absolute minima are:

$$\begin{aligned} 0 < \delta_f < \delta_f^{c1}, \quad \theta_m = \pi \\ \delta_f^{c2} < \delta_f < \pi, \quad \theta_m = 0. \end{aligned} \quad (20)$$

However, as mentioned above for $\theta_m = 0, \pi$, $U^{sym} = (I, -I)$ and those lie in the center of $SU(2)$, thus the symmetry is not broken.

Next, we would like to determine the regions of δ_f , in which $\theta = 0, \pi$ are the absolute minima, respectively. For this purpose, in Figure 10, and Figure 11, we have plotted $c_1 V_f(\theta, N_f = 1, z_f = 0, \delta_f)$, with respect to θ , for selected values of δ_f , in the $0 < \delta_f < \pi/2$, and $\pi/2 < \delta_f < \pi$ intervals, respectively.

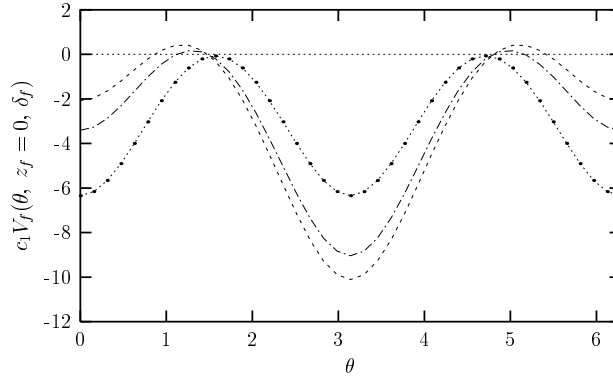


Figure 9: The dependence on θ of $c_1 V_f(\theta, N_f = 1, z_f = 0, 0 < \delta_f < \pi/2)$. Here, $\delta_f = 0$, and $\delta_f = \pi/4$ for the bottom and the middle curves, respectively, whereas $\delta_f = \pi/2$ for the top curve.

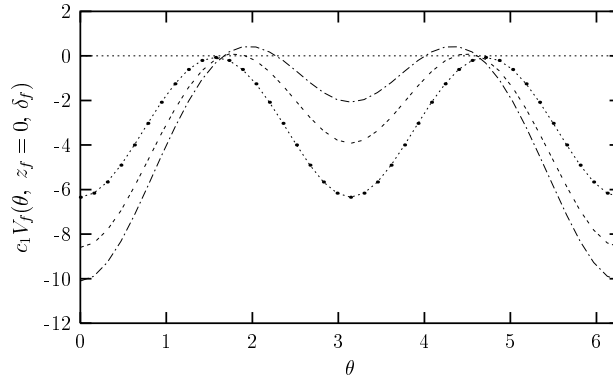


Figure 10: The dependence on θ of $c_1 V_f(\theta, N_f = 1, z_f = 0, \pi/2 < \delta_f < \pi)$. Here, $\delta_f = 7\pi/10$ and $\delta_f = \pi$ for the middle and top curves, respectively, whereas $\delta_f = \pi/2$ for the bottom curve.

We see from Figure 9, and 10 that $\theta = 0, \pi$ are the absolute minima for $\pi/2 < \delta_f$, and $\pi/2 < \delta_f < \pi$ respectively, as in the case discussed by Hosotani [2], and they are degenerate at

$\delta_f = \pi/2$. However, for $\theta_m = 0, \pi$, $U^{sym} = (I, -I)$ and these lie in the center of $SU(2)$, thus the symmetry is not broken.

Similar pattern can be obtained for the behaviour of $V_f(\theta, N_f = 4, z_f = 0, \delta_f)$ case. We have observed that the secondary local minima become shallower (that is smoothed out), however, with increasing N_f .

Next, we have to check the stability properties of the absolute minima under the variation of $V_f''(\theta, N_f, z_f, \delta_f)$ with respect to z_f . Using (16), we get:

$$\begin{aligned} c_2 V_f''(\theta = 0, N_f, z_f, \pi/2 < \delta_f < \pi) &= \sum_{n=1} \frac{1}{n^3} \left[3 - N_f F(z_f n) \cos n\delta_f \right], \\ c_2 V_f''(\theta = \pi, N_f, z_f, 0 < \delta_f < \pi/2) &= \sum_{n=1} \frac{1}{n^3} \left[3 - (-1)^n N_f F(z_f n) \cos n\delta_f \right], \end{aligned} \quad (21)$$

and look for the critical values of z_f , where $c_2 V_f''(\theta = 0, N_f, z_f, \pi/2 < \delta_f < \pi)$, and $c_2 V_f''(\theta = \pi, N_f, z_f, 0 < \delta_f < \pi/2)$ change sign, in Figure 11 and Figure 12, respectively, when $N_f = 1$.

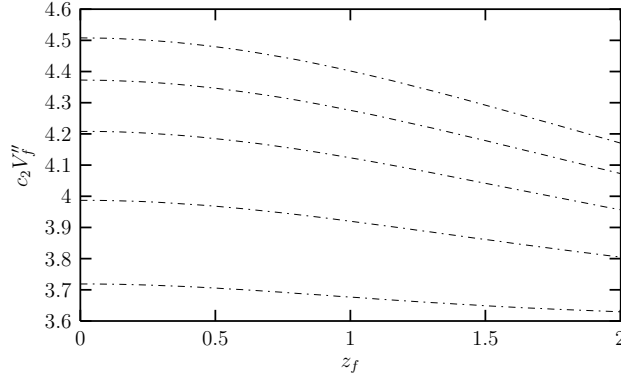


Figure 11: The dependence on z_f of $c_2 V_f''(\theta = 0, N_f = 1, z_f, \pi/2 < \delta_f < \pi)$. Here, $\delta_f = \pi$ for the top curve, whereas $\delta_f = \pi/2$ for the bottom curve. For the curves in between $\delta_f = 6\pi/10, 7\pi/10, 8\pi/10$, from bottom to top, respectively.

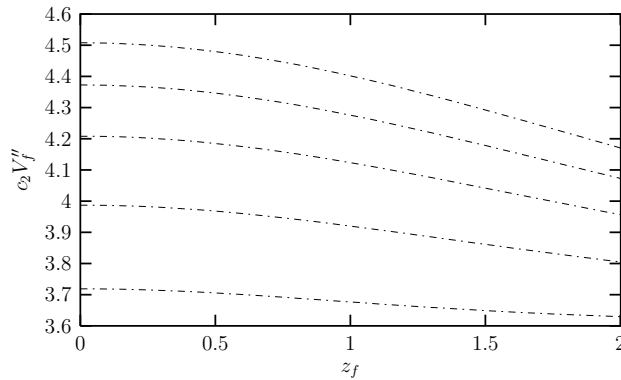


Figure 12: The dependence on z_f of $c_2 V_f''(\theta = \pi, N_f = 1, z_f, 0 < \delta_f < \pi/2)$. Here, $\delta_f = 0$ for the top curve, whereas $\delta_f = \pi/2$, for the bottom curve. For the curves in between $\delta_f = 2\pi/10, 3\pi/10, 4\pi/10$, from bottom to top, respectively.

Note that the plots in Figure 11 and Figure 12 are identical despite the fact that the intervals for δ_f are different. This is due to the fact that $V_f''(\theta = 0, N_f, z_f, \delta_f) \rightarrow V_f''(\theta = \pi, N_f, z_f, \delta_f)$ under the transformation $\delta_f \rightarrow \delta_f - \pi$.

A comparative analysis of Figure 11 and Figure 12 shows that $V_f''(\theta, N_f = 1, z_f, \delta_f)$ is always positive independent of z_f ; that is there are no critical values for z_f .

Now, we would like to study the behaviour of $V_f(\theta)$ under the variations of z_f . In Figure 13, we have plotted $V_f(\theta, z_f)$ for selected values of δ_f from the region in which $\theta = 0$, and π are global minima for $z_f = 0$, respectively.

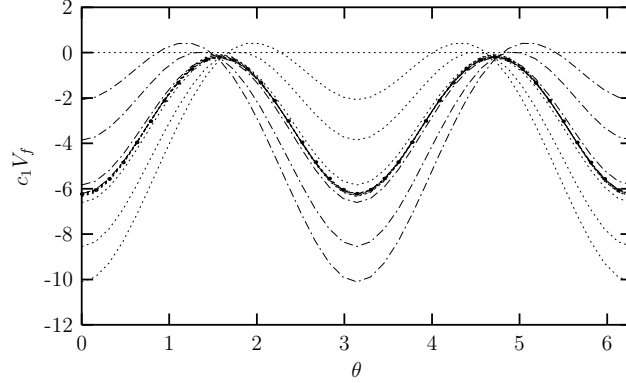


Figure 13: The dependence on θ of $c_1V_f(\theta, N_f = 1, z_f, \delta_f)$. Here, $\delta_f = 0$, and $\delta_f = \pi$ are represented by the dot-dashed curves, and dotted curves, respectively. The dot-dashed curves (with $\delta_f = 0$), from bottom to top, are for $z_f = 0$, $z_f = 2$, and $z_f = 5$, whereas the dotted curves (with $\delta_f = \pi$), from top to bottom, are for $z_f = 0$, $z_f = 2$, and $z_f = 5$. When $z_f = 8$, all the curves coagulate to the same limiting degenerate minima curve (shown by dots in the middle), which always happens at $\delta_f = \pi/2$.

We would like to note that, in Figure 13 we have shown the curves for the values of $z_f = 0$, $z_f = 2$, and $z_f = 5$ only, as they are very densely packed and very difficult to distinguish from each other in the region $5 < z_f < 8$.

We have observed that for $z_f = 8$, all the curves coagulate to the same limiting curve, corresponding to the degenerate minima ($\delta_f = \pi/2$).

Thus, $z_f = 8$ emerges as some sort of critical value, not in the sense that we move from one global minimum to another, when we cross it; but which ever local minimum we start from, we end up with the degenerate minima case, when we reach this value of z_f . As the local minima are always either one of the $\theta = 0, \pi$, then there is no change in the symmetry pattern.

Finally, we look at the variation of $V_f''(\theta_m, N_f, z_f, \delta_f)$ in the specific intervals of δ_f found above, for $N_f = 4$: For this purpose, in Figure 14 and Figure 15 we analyze the dependence of $c_2V_f''(\theta = 0, N_f = 4, z_f, \delta_f)$ on z_f in the $\delta_f^{c_2} = 2.61 < \delta_f < \pi$ and $0 < \delta_f < \delta_f^{c_1} = 0.53$ intervals, respectively, for selected values of δ_f .

Note that Figure 14 and Figure 15 show the same symmetry behaviour we mentioned above, in relation to the Figure 11 and Figure 12.

A comparative analysis of Figure 14 and Figure 15 suggest that the variation of $V_f''(\theta, N_f = 4, z_f, \delta_f)$ at $\theta = 0, \pi$ with respect to z_f , show similar behaviour to those of $N_f = 1, 2$. Thus, once we restrict δ_f to the allowed range in this case, mass does not play any further role.

In summary the above detailed analysis shows that fundamental fermions do not break $SU(2)$ symmetry, irrespective of the values of the parameters δ_f , z_f , and N_f .

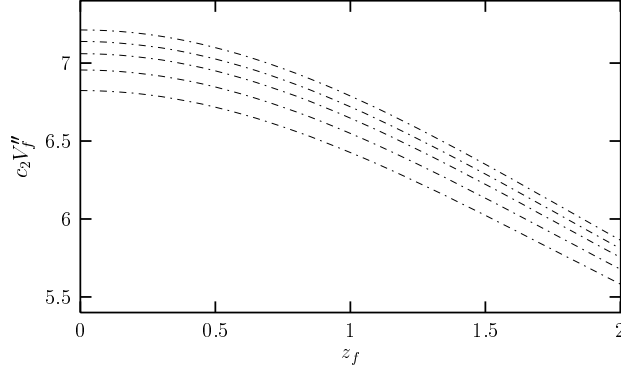


Figure 14: The dependence on z_f of $c_2V_f''(\theta = 0, N_f = 4, z_f, \delta_f^{c_2} < \delta_f < \pi)$. Here, $\delta_f = \pi$ for the top curve, whereas $\delta_f = 2.61$, for the bottom curve. For the curves in between, $\delta_f=2.91, 2.81, 2.71$, from bottom to top, respectively.

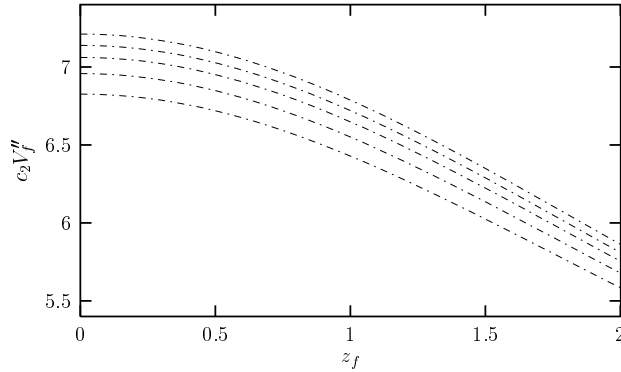


Figure 15: The dependence on z_f of $c_2V_f''(\theta = \pi, N_f = 4, z_f, 0 < \delta_f < \delta_f^{c_1})$. Here, $\delta_f = 0$ for the top curve, whereas $\delta_f = 0.53$, for the bottom curve. For the curves in between, $\delta_f=0.23, 0.33, 0.43$, from top to bottom, respectively.

5 Fundamental and Adjoint Fermions with equal masses

With these inputs in mind, let us look at the general case where there are N_a massive adjoint fermions, and N_f massive fundamental fermions with equal masses ($z_a = z_f = z$).

The potential is given by:

$$\begin{aligned}
 V_{af}(\theta, N_a, N_f, z, \delta_a, \delta_f) &= \frac{1}{c_1} \sum_{n=1} \frac{1}{n^5} \left\{ \left[-3 + 4 N_a F(zn) \cos n\delta_a \right] \left(1 + \cos 2n\theta \right) \right. \\
 &\quad \left. + 4 N_f F(zn) \cos n\delta_f \cos n\theta \right\}. \tag{22}
 \end{aligned}$$

The most trivial roots of V'_{af} are $\theta = 0, \pi$. In principle, there could be non-trivial roots of $V'_{af} = 0$ as well, depending on the values of the parameters; we checked this numerically, and analytically, and have shown that there are no other minima. Again, as in the previous special cases we look at the two special limits, namely $z_a = z_f \rightarrow \infty$, and $z_a = z_f \rightarrow 0$.

One first notes that for $m_a = m_f \rightarrow \infty$, $F(zn) \rightarrow 0$ which means $V \rightarrow V_{\text{pure gauge}}$, as all fermions, adjoint and fundamental, decouple (thus, as before $\theta = 0 \pmod{\pi}$ is an absolute minimum). For $m_a = m_f \rightarrow 0$, $F(zn) \rightarrow 1$, and

$$c_2 V''_{af}(\theta = 0, N_a, N_f, z = 0, \delta_a, \delta_f) = \sum_{n=1} \frac{1}{n^3} \left(3 - 4 N_a \cos n\delta_a - N_f \cos n\delta_f \right),$$

$$c_2 V''_{af}(\theta = \pi, N_a, N_f, z = 0, \delta_a, \delta_f) = \sum_{n=1} \frac{1}{n^3} \left(3 - 4 N_a \cos n\delta_a - N_f (-1)^n \cos n\delta_f \right). \quad (23)$$

To determine the ranges of δ_f, δ_a , we first plot the $\delta_f - \delta_a$ region, for which $c_2 V''_{af}(\theta = 0, N_a, N_f, z = 0, \delta_a, \delta_f) > 0$ in Figure 16, when $N_a = N_f = 1$.

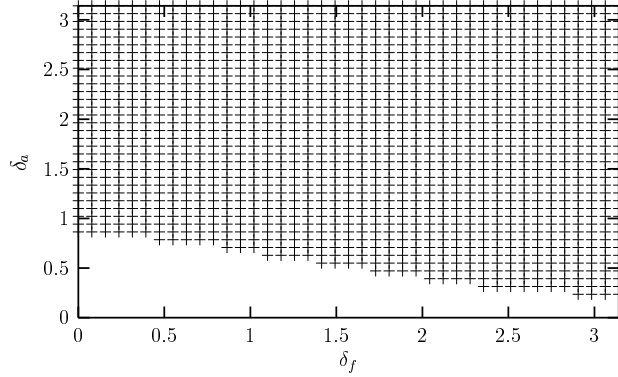


Figure 16: The $\delta_f - \delta_a$ region, for which $c_2 V''_{af}(\theta = 0, N_a = N_f = 1, z = 0, \delta_a, \delta_f) > 0$.

As can be observed from Figure 16 that the lower bound of δ_a ranges from $\delta_a = 3\pi/40$, up to $\delta_a = \pi/4$, when δ_f changes from 0 to π . One notes that the lower bound of δ_f ranges from $3\pi/20$ to $37\pi/40$, in the $3\pi/40 \lesssim \delta_a \lesssim \pi/4$, interval. On the other hand, for $10\pi/40 < \delta_a < \pi$, there is no constraint on δ_f ; That is, all values of δ_f are allowed for $\delta_a > 10\pi/40$.

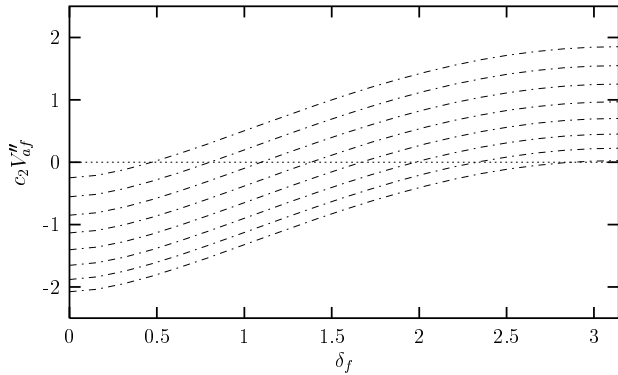


Figure 17: The dependence on δ_f of $c_2 V''_{af}(\theta = 0, N_a = N_f = 1, z = 0, \delta_a, \delta_f)$, for $3\pi/40 \lesssim \delta_a \lesssim \pi/4$. Here, $\delta_a = \pi/4$ for the top curve, whereas $\delta_a = 3\pi/40$, for the bottom curve. In the remaining portion of the parameter space, namely $\delta_a < 3\pi/40$, and $\delta_a > \pi/4$, $c_2 V''_{af}$ does not change sign.

In Figure 17 we plot $c_2 V''_{af}(\theta = 0, N_a = N_f = 1, z = 0, \delta_a, \delta_f)$ with respect to δ_f , for the set of values $3\pi/40 \lesssim \delta_a \lesssim \pi/4$, for which $c_2 V''_{af}(\theta = 0, N_a = N_f = 1, z = 0, \delta_a, \delta_f)$ was changing sign in Figure 16. Here, $\delta_a = \pi/4$ for the top curve, whereas $\delta_a = 3\pi/40$ for the bottom curve.

As can be seen from Figure 17 that when $\delta_a = \pi/4$, $c_2V''_{af}(\theta = 0, N_a = N_f = 1, z = 0, \delta_a, \delta_f)$ changes sign at $\delta_f = 3\pi/20$, whereas for $\delta_a = 3\pi/40$, the lower bound on δ_f moves to $\delta_f = 37\pi/40$. For $\delta_a > \pi/4$, $c_2V''_{af}(\theta = 0, N_a = N_f = 1, z = 0, \delta_a, \delta_f)$ does not change sign for any value of δ_f , which is consistent with Figure 16.

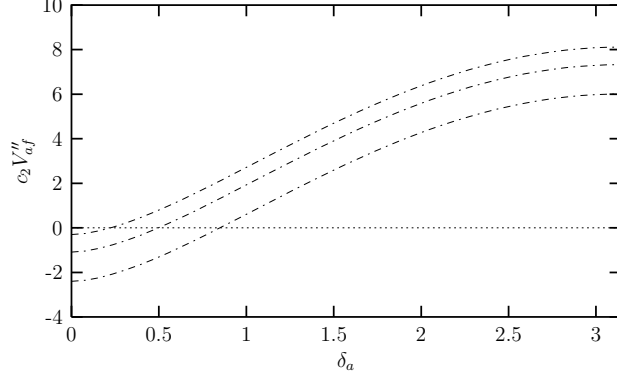


Figure 18: The dependence on δ_a of $c_2V''_{af}(\theta = 0, N_a = N_f = 1, z = 0, \delta_a, \delta_f)$. Here, $\delta_f = \pi$, $\delta_f = \pi/2$ and $\delta_f = 0$, for the top, middle, bottom curves, respectively. $c_2V''_{af}$ changes sign for all values of δ_f ; the critical values of δ_a decrease with increasing values of δ_f .

In Figure 18, we analyze the dependence on δ_a of $c_2V''_{af}(\theta = 0, N_a = N_f = 1, z = 0, \delta_a, \delta_f)$ for given values of δ_f , namely $\delta_f = \pi$ (top curve), $\delta_f = \pi/2$ (middle curve), and $\delta_f = 0$ (bottom curve).

As can be seen from Figure 18, $c_2V''_{af}(\theta = 0)$ changes sign for all values of δ_f , whereas the lower bound on δ_a moves from $\pi/4$ to $3\pi/40$, with the increasing values of δ_f . For instance, when $\delta_f = 0$ the lower bound on δ_a , at which the $c_2V''_{af}$ changes sign, is $\delta_a = \pi/4$, whereas for $\delta_f = \pi$, it is $\delta_a = 3\pi/40$, which is consistent with Figure 16.

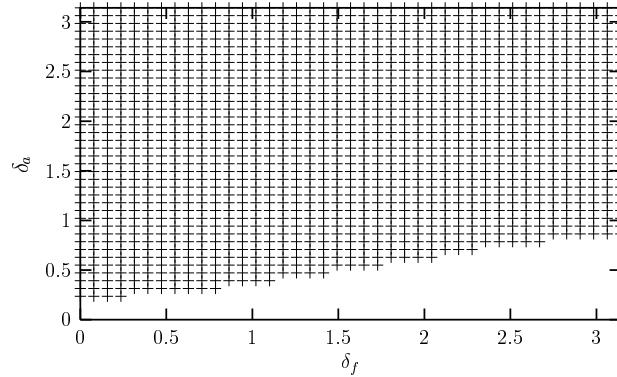


Figure 19: The δ_f - δ_a region, for which $V''_{af}(\theta = \pi, N_a = N_f = 1, z = 0, \delta_a, \delta_f) > 0$.

In Figure 19, we plot the δ_f - δ_a region, for which $c_2V''_{af}(\theta = \pi, N_a = N_f = 1, z = 0, \delta_a, \delta_f) > 0$. Here, all values of δ_f from 0 to π are allowed above the critical value $\delta_a > \pi/4$, as was the case in Figure 16, also.

In Figure 20, we plot $c_2V''_{af}(\theta = \pi, N_a = N_f = 1, z = 0, \delta_a, \delta_f)$ with respect to δ_f , for the set of values $3\pi/40 \lesssim \delta_a \lesssim \pi/4$, in the region where $c_2V''_{af}(\theta = \pi, N_a = N_f = 1, z = 0, \delta_a, \delta_f)$

was changing sign in Figure 19. In Figure 20, the top and the bottom curves represent $\delta_a = \pi/4$, and $\delta_a = 3\pi/40$, respectively. One notes that $c_2V''_{af}(\theta = \pi, N_a = N_f = 1, z = 0, \delta_a, \delta_f)$ does not change sign in the remaining portion of the δ_a -parameter space (namely, for $\delta_a < 3\pi/40$, and $\delta_a > \pi/4$).

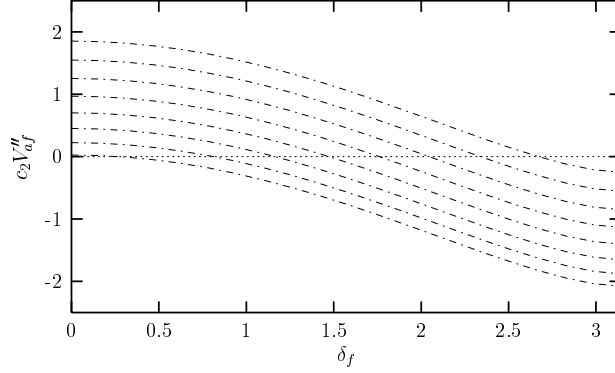


Figure 20: The dependence on δ_f of $c_2V''_{af}(\theta = \pi, N_a = N_f = 1, z = 0, \delta_a, \delta_f)$, for the set of values $3\pi/40 \lesssim \delta_a \lesssim \pi/4$. Here, $\delta_a = \pi/4$ for the top curve, whereas $\delta_a = 3\pi/40$, for the bottom curve. In the remaining portion of the δ_a -parameter space $c_2V''_{af}$ does not change sign.

In Figure 21, we analyze the dependence on δ_a of $c_2V''_{af}(\theta = \pi, N_a = N_f = 1, z = 0, \delta_a, \delta_f)$ for given values of δ_f when $N_f = N_a = 1$. In the Figure, the top, middle, bottom curves represent $\delta_f = 0, \delta_f = \pi/2$ and $\delta_f = \pi$, respectively. Similar to observations made for Figure 20, when $\delta_f = \pi$, the potential changes sign at $\delta_f = \pi/4$, whereas for $\delta_f = 0$, the lower bound on δ_a is $\delta_f = 3\pi/40$, which is consistent with Figure 19.

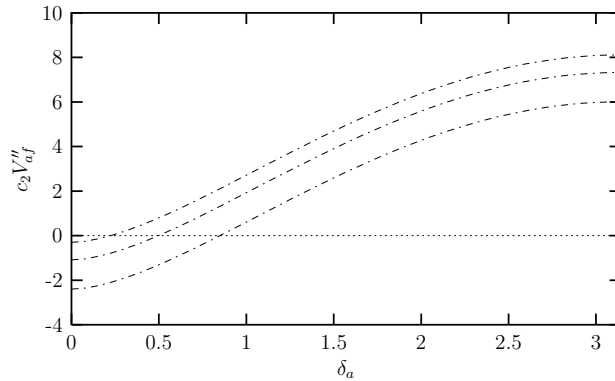


Figure 21: The dependence on δ_a of $c_2V''_{af}(\theta = 0, N_a = N_f = 1, z = 0, \delta_a, \delta_f)$. Here, $\delta_f = \pi, \delta_f = \pi/2$ and $\delta_f = 0$, for the top, middle and the bottom curves, respectively.

We have to next check the region of $\delta_a - \delta_f$ for which $\theta = 0, \pi$ are the absolute minima. For this purpose, in Figure 22 we have plotted $c_2V_{af}(\theta, N_a = N_f = 1, z = 0, \delta_a, \delta_f)$, with respect to θ for selected values of $\delta_a > \delta_a^{cr} = \pi/4$, identified in Figure 16 and Figure 19 for both $\theta = 0$, and π .

It is seen from Figure 22 that $\theta = 0$ is the absolute minimum for $\pi/2 < \delta_f < \pi$, whereas $\theta = \pi$ is the absolute minimum for $0 < \delta_f < \pi/2$, as in the pure fundamental fermions case. Note that these are degenerate at $\delta_f = \pi/2$. However, as before irregardless of which one of $\theta = 0, \pi$ are the

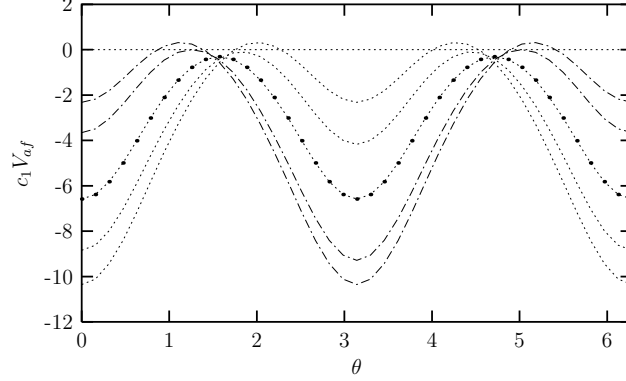


Figure 22: The dependence of $c_1V_{af}(\theta)$, $N_a = N_f = 1$, $z = 0$, $\delta_a = \pi/2$, δ_f on θ . Here, the dotted-line in the middle is for $\delta_f = \pi/2$. The upper two lines, from top to bottom, are for $\delta_f = \pi$, and $\delta_f = 7\pi/10$, respectively, chosen in the $\pi/2 < \delta_f < \pi$ interval. The lower two lines are for, from bottom to top, $\delta_f = 0$, and $\delta_f = \pi/4$, respectively, chosen in the $0 < \delta_f < \pi/2$ interval.

absolute minima, the symmetry is unbroken, provided that $\delta_a > \delta_a^{cr} = \pi/4$.

Similar analysis can be made for $c_1V_{af}(\theta)$, $N_a = N_f = 1$, $z = 0$, $\delta_a, \delta_f = \pi/2$, for selected values of δ_a , chosen from the region $\delta_a > \delta_a^{cr} = \pi/4$. We see that in this case $\theta = 0, \pi$ are the degenerate absolute minima, which is consistent with the remarks of Figure 16 and Figure 19.

Next, we would like to adress the issue of stability of these absolute minima, we have found for the massless case, under the variations of z .

We have previously observed that there were critical values of z , at which symmetry pattern changed, for the adjoint case. But in the fundamental fermions case the mass did not play any role on the symmetry pattern. In the present case, that is when the fundamental and adjoint fermions exist together (with equal masses), we would like to check which behaviour of the previous special cases would be carried over.

We get from Eq. (22):

$$\begin{aligned}
c_2V_{af}''(\theta = 0, N_a, N_f, z, \delta_a, \delta_f) &= \sum_{n=1} \frac{1}{n^3} \left(3 - 4 N_a F(zn) \cos n\delta_a \right. \\
&\quad \left. - N_f F(zn) \cos n\delta_f \right), \\
c_2V_{af}''(\theta = \pi, N_a, N_f, z, \delta_a, \delta_f) &= \sum_{n=1} \frac{1}{n^3} \left(3 - 4 N_a F(zn) \cos n\delta_a \right. \\
&\quad \left. - N_f (-1)^n F(zn) \cos n\delta_f \right). \tag{24}
\end{aligned}$$

In Figure 23, and Figure 24, we plot the 3-dimensional graphs depicting $c_2V_{af}''(\theta = 0, N_a = N_f = 1, z, \delta_a, \delta_f)$, against $\delta_a - z$, and $\delta_f - z$, when $\delta_a - \delta_f$ are restricted to the region where $\theta = 0$ was a minimum in the massless case.

In Figure 23, we obtain 3-dimensional surfaces for each value of δ_f , which we choose within the interval $[0, \pi]$. For instance the top surface corresponds to $\delta_f = \pi$, whereas the bottom one represents $\delta_f = 0$. One notes that for $\delta_f = 0$, the lowest allowed bound of δ_a is $\delta_a = 11\pi/40$, consistent with Figure 16.

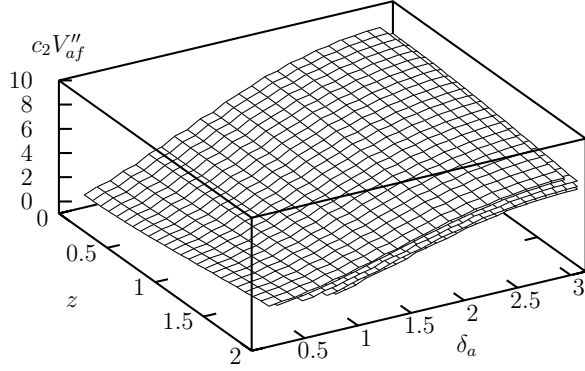


Figure 23: The dependence of $c_2V''_{af}(\theta = 0, N_a = N_f = 1, z, \delta_a, \delta_f)$ on δ_a and z , for selected values of δ_f . Here, δ_a and δ_f values are restricted to the shaded region in Figure 16.

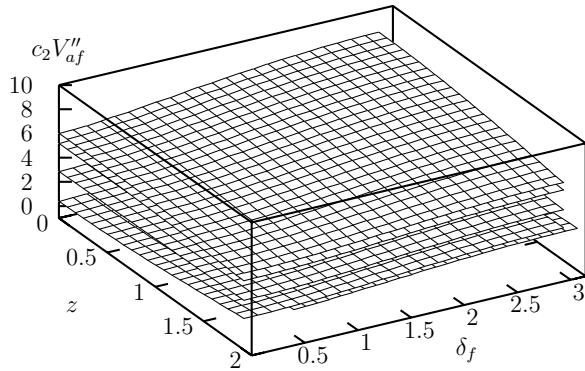


Figure 24: The dependence of $c_2V''_{af}(\theta = 0, N_a = N_f = 1, z, \delta_a, \delta_f)$ on δ_f and z , for selected values of δ_a . Here, δ_a and δ_f values are restricted to the shaded region in Figure 16.

Similarly, each three dimensional surface in Figure 24 corresponds to a discrete value of δ_a changing in the $[0, \pi]$ interval. Here, the bottom surface represents $\delta_a = \pi/4$, at which case the lowest allowed bound on δ_f is $\delta_f = 3\pi/20$, as in Figure 16.

A comparative analysis of Figure 23 and Figure 24 shows that $c_2V''_{af}(\theta = 0, N_a = N_f = 1, z, \delta_a, \delta_f)$, does not change sign with the variations of z , when δ_a , and δ_f are restricted to the shaded region in Figure 16. That is $\theta = 0$ remains as a minimum independent of the values of z .

To address the stability issue of the minimum $\theta = \pi$, we plotted a similar set of 3-dimensional graphs depicting $c_2V''_{af}(\theta = \pi, N_a = N_f = 1, z, \delta_a, \delta_f)$, against $\delta_a - z$ in Figure 25, and $\delta_f - z$ in Figure 26, where δ_a and δ_f values are restricted to the shaded region in Figure 19.

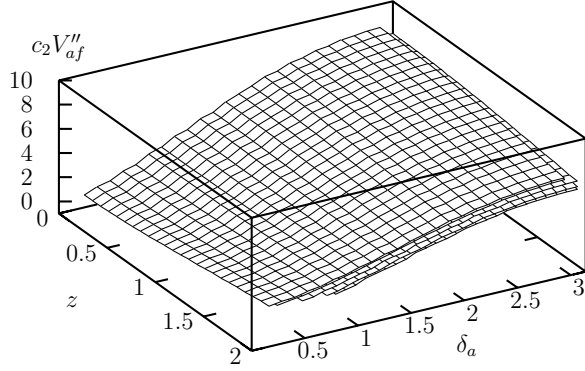


Figure 25: The dependence of $c_2V''_{af}(\theta = \pi, N_a = N_f = 1, z, \delta_a, \delta_f)$, on δ_a and z , for selected values of δ_f . Here, δ_a and δ_f values are restricted to the shaded region in Figure 19.

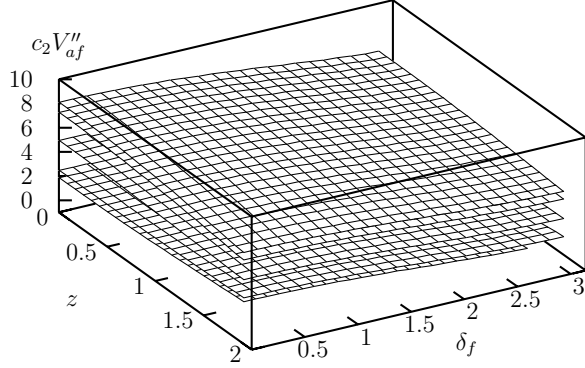


Figure 26: The dependence of $c_2V''_{af}(\theta = \pi, N_a = N_f = 1, z, \delta_a, \delta_f)$, on δ_f and z , for selected values of δ_a . Here, δ_a and δ_f values are restricted to the shaded region in Figure 19.

In Figure 25, the top surface corresponds to $\delta_f = 0$, and the bottom one represents $\delta_f = \pi$, whereas in Figure 26, the top surface corresponds to $\delta_a = \pi$, and the bottom one to $\delta_a = \pi/4$.

A comparative analysis of Figure 25 and Figure 26 shows that $c_2V''_{af}(\theta = \pi, N_a = N_f = 1, z, \delta_a, \delta_f)$ does not change sign, and always stays positive, independent of the values of z , in the allowed region of $\delta_a - \delta_f$.

Now, we would like to investigate the special case in which $\theta = 0$ and $\theta = \pi$ minima are degenerate which can be checked easily to occur for $\delta_f = \pi/2$, and $\delta_a > \delta_a^{cr}$. The result is depicted in Figure 27, where we plot $c_2V''_{af}(\theta = 0 \text{ [mod}\pi], N_a = N_f = 1, z, \delta_a, \delta_f)$ with respect to z for $\delta_f = \pi/2$, and for the selected set of values of δ_a within the allowed range; $\delta_a > \delta_a^{cr} = \pi/4$. Namely, we choose $\delta_a = \pi$ (top curve), $\delta_a = 3\pi/2$ (middle curve), $\delta_a = \pi/2$ (bottom curve).

We see that for this special regime of the parameters, namely $\delta_f = \pi/2, \delta_a > \delta_a^{cr}$, $V''_{af}(\theta = 0, \pi)$ is always positive (does not change sign) with the variations of z .

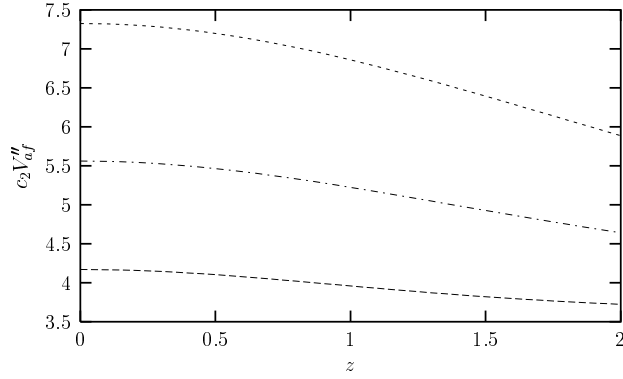


Figure 27: The dependence on z of $c_2V''_{af}(\theta = 0 \pmod{\pi}, N_a = N_f = 1, z, \delta_a, \delta_f)$ when $\delta_f = \pi/2$, for the selected set of values of δ_a : $\delta_a = \pi$ (top curve), $\delta_a = 3\pi/2$ (middle curve), $\delta_a = \pi/2$ (bottom curve).

Lastly, we would like to study the behaviour of the effective potential under the variations of z . For this purpose, in Figure 28, we have plotted $V_{af}(\theta, z)$ for selected characteristic values of δ_a and δ_f picked from Figure 22 (which in turn identified from Figure 16 and 19), defining the allowed regions of the parameter space for the local minima $\theta_m = 0, \pi$.

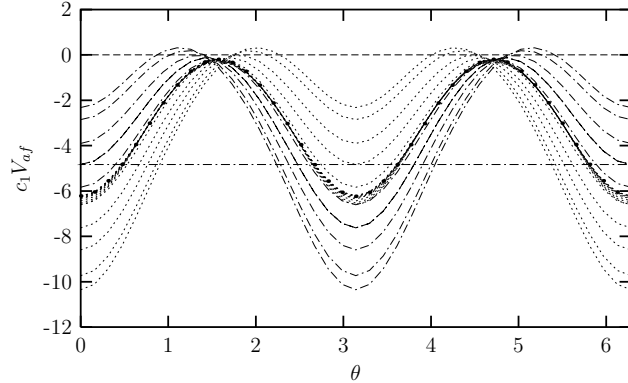


Figure 28: The dependence on θ of V_{af} when $N_f = 1, N_a = 1$, for the cases $\delta_a = \pi/2, \delta_f = \pi/2$ (shaded region), $\delta_a = \pi/2, \delta_f = 0$ (dot-dashed curves), $\delta_a = \pi/2, \delta_f = \pi$ (dotted curves). Here, the dot-dashed lines, from bottom to top, are for $z = 0, z = 1, z = 2, z = 3, z = 5$. The dotted lines, from top to bottom, are for $z = 0, z = 1, z = 2, z = 3, z = 5$. Again when $z_f = 8$, all the curves coagulate to the same limiting degenerate minima curve (shown by dots on the edge of the shaded region), which always happens at $\delta_f = \pi/2$, irregardless of the values of δ_a .

We see from Figure 28 that, for the pair $\delta_a = \pi/2, \delta_f = \pi$, we get the dotted curves for the values of $z = 0, z = 1, z = 2, z = 3, z = 5$, from top to bottom, with the global minimum $\theta_m = 0$. Similarly, for $\delta_a = \pi/2, \delta_f = 0$, we obtain the dot-dashed curves for the values of $z = 0, z = 1, z = 2, z = 3, z = 5$, from bottom to top, with the global minimum $\theta_m = \pi$.

We see that these two groups of curves (with $\theta_m = 0$, and $\theta_m = \pi$, respectively) all coagulate to the limiting curve shown by dots on the edge of the shaded region, which corresponds to the degenerate minima case (for $\delta_f = \pi/2$ irregardless of the values of δ_a).

Thus $z = 8$ emerges as some critical value, not in the sense that we move from one global minimum to another, when we cross this value; but whichever local minimum we start from (in the massless case) we end up with the degenerate minima case when we reach this value of z , as in the pure fundamental fermions case. As the absolute minima are always either one of the $\theta = 0, \pi$, then there is no change in symmetry pattern as a consequence of this rather intricate dynamical phenomenon.

The above detailed analysis shows that the absolute minima of the massless case, namely $\theta = 0$ or $\theta = \pi$ are unaffected, and the $SU(2)$ symmetry is unbroken by the fermion masses, a behaviour we are familiar with from the special case of pure fundamental fermions. Furthermore, this result is self-consistent, as we have the same minima and thus the same symmetry pattern in the $m \rightarrow 0$, and $m \rightarrow \infty$ cases. That is the fundamental fermions play a more dominant role than the adjoint ones in determining the symmetry pattern.

6 Conclusions

In this work, we have constructed the effective potential for the Wilson loop in the $SU(2)$ gauge theory with N_f massive fundamental and N_a massive adjoint fermions on $S^1 \times M^4$ in the one-loop level, assuming periodic boundary condition for the gauge field, and the general boundary conditions for fermions with arbitrary phase, and investigated the symmetry structure of the vacuum.

Our results can be summarized as follows:

(i) For the adjoint fermions, the symmetries of the system depend critically on both the bulk mass and the bc parameters. We have considered the special limits of the general case, namely the regime of Hosotani with massless fermions and arbitrary boundary conditions, that of Takenaga with massive fermions and periodic boundary conditions ($\delta_a = 0$), and that of Davies and McLachan (the simplest of them all) with massless fermions, and periodic boundary conditions. Our predictions are identical to theirs in the corresponding limits. We have further observed an interesting phenomenon, that for a special value of δ_a (namely, $\delta_a = 0.71$, when $N_a = 1$) both broken and unbroken phases coexist for $z_a \leq 0.7$. Further analysis of this phenomenon is postponed to a future work.

(ii) Fundamental fermions can never lead to a spontaneous breakdown of the gauge symmetry irrespective of the values of the parameters z_f , δ_f , and N_f .

(iii) When there are fundamental and adjoint fermions together (with equal masses), we first note that in the massless case there are critical values for the boundary condition parameters δ_a and δ_f , in deciding the absolute minima. However as these are either one of $\theta_m = 0, \pi$, the symmetry is intact irregardless of their preferences. Thus there are no critical values for the bc parameters as far as symmetry breaking pattern is concerned. We further checked the role played by the masses on the symmetry pattern. We have observed that the minimum values of the effective potential change with the variations of z , however not as much to change the global minimum from $\theta_m = 0$ to $\theta_m = \pi$, or vice-versa. There is a special value of z , $z = 8$, at which all the curves coagulate to the same limiting degenerate minima (which always happens at $\delta_f = \pi/2$). However, as the absolute minima are always either one of the $\theta_m = 0, \pi$, the $SU(2)$ symmetry remains intact independent of the masses, provided that the boundary condition parameters are chosen within the allowed region of the massless regime. It is interesting that the fundamental fermions play a more dominant role on the gauge symmetry pattern than the adjoint ones, when they act together, as the result is identical to the pure fundamental fermions case.

As explained in the introduction, one immediate application of the aforementioned compactification is to use $\theta(x)$ as inflaton. The cosmological data require the inflaton potential to be rather smooth and inflaton itself to take super-Planckian values. This necessitates the extension

of field-theoretic description of Nature into string territory which is hardly acceptable. However, as already pointed out in [8, 9] and extended to massive bulk fields in [10], the non-integrable phase $\theta(x)$ is a perfect inflaton candidate due to its shift symmetry (as implied by the higher dimensional gauge invariance). The novelty provided by our analysis is that possible symmetry breaking parameter domains are identified, and thus, the theory below $1/R$ might look like either as an Abelian or non-Abelian theory. In each case, experimentally favoured four-dimensional gauge coupling $g_4(1/R) \sim 10^{-3}$ [8, 9] experiences different constraints from experimental data at the weak scale.

Another point which might be of phenomenological importance concerns the creation of Q balls. Indeed, the four-dimensional effective theory for the non-integrable phase possesses either and Abelian or non-Abelian invariance, and in either case its self-interactions generate lumps of $\theta(x)$ matter in which all symmetries are broken [11, 12]. These lumps of matter are perfect dark matter candidates. Here one notices that such Q-balls differ from the Kaluza-Klein Q-balls of [13] in that the latter rests on the inclusion of all Kaluza-Klein modes whereas the former is based on only $\theta(x)$ which is the zero-mode of $A_5(x, y)$. The stability as well as further characteristics of Q-balls of non-integrable phase factor need further analysis of (5).

We would like to thank Durmuş A. Demir for extremely helpful discussions.

References

- [1] Y. Aharonov and D. Bohm, Phys. Rev. **115** (1959) 485.
- [2] Y. Hosotani, Phys. Lett. B **126** (1983) 309.
- [3] A. Higuchi and L. Parker, Phys. Rev. D **37** (1988) 2853.
- [4] A. T. Davies and A. McLachlan, Phys. Lett. B **200** (1988) 305.
- [5] Y. Hosotani, Annals Phys. **190** (1989) 233.
- [6] K. Takenaga, Phys. Lett. B **570** (2003) 244 [arXiv:hep-th/0305251].
- [7] P. Candelas, G. T. Horowitz, A. Strominger and E. Witten, Nucl. Phys. B **258** (1985) 46; J. D. Breit, B. A. Ovrut and G. Segre, Phys. Lett. B **162** (1985) 303.
- [8] N. Arkani-Hamed, H. C. Cheng, P. Creminelli and L. Randall, Phys. Rev. Lett. **90** (2003) 221302 [arXiv:hep-th/0301218].
- [9] N. Arkani-Hamed, H. C. Cheng, P. Creminelli and L. Randall, JCAP **0307** (2003) 003 [arXiv:hep-th/0302034].
- [10] L. Pilo, D. A. J. Rayner and A. Riotto, Phys. Rev. D **68** (2003) 043503 [arXiv:hep-ph/0302087].
- [11] S. R. Coleman, Nucl. Phys. B **262** (1985) 263 [Erratum-ibid. B **269** (1986) 744];
- [12] A. Kusenko, Phys. Lett. B **404** (1997) 285 [arXiv:hep-th/9704073].
- [13] D. A. Demir, Phys. Lett. B **495** (2000) 357 [arXiv:hep-ph/0006344].